

# Thermoresponsive Hydrogels as Microniches for Growth and Controlled Release of Induced Pluripotent Stem Cells

Wanjuan Liang, Sumati Bhatia, Felix Reisbeck, Yinan Zhong, Abhishek Kumar Singh, Wenzhong Li,\* and Rainer Haag\*

The recently emerging stem-cell artificial niche engineering in induced pluripotent stem cell (iPSCs) 3D cultures has provided enormous opportunities to fully utilize the potential of these cells in biomedical applications. Although a fully chemically defined niche environment can supply cells with desirable safety for clinical use, establishing an artificial degradable niche environment for the controlled release of proliferated cells under mild conditions is still a big challenge. Here, an advanced controlled releasable iPSC 3D artificial niche is reported based on dendritic polyglycerol and poly(*N*-isopropylacrylamide)-*co*-polyethylene glycol polymers via a physical–chemical cogelation strategy. Benefiting from the chemically defined synthetic materials and their precise cooperation by covalent cross-linking and physical phase transition, the cogelation-based artificial niche system can be adjusted with optimal parameters and owns high cell biocompatibility to support the robust production of high quality iPSCs with an excellent expansion efficiency. Moreover, the expanded cells can be released out of their niche environment controllably only by adjusting the temperature. Overall, this controlled release hydrogel scaffold shows great promise in iPSC 3D culture for downstream applications.

prominent ethical problems.<sup>[2,5]</sup> They are serving as a powerful tool in numerous applications.<sup>[6–11]</sup> However, it should be noted that large amounts of cells with high quality are needed during most of the applications.<sup>[12,13]</sup> For example, at least  $10^8$ – $10^{10}$  cells are required per patient in the most current cell therapy protocols and those under development.<sup>[14]</sup> The therapeutic use of the iPSCs cells, therefore, greatly necessitates their efficient expansion in large scale under safety-reliable and well-defined culture conditions.

Actually, since the discovery of iPSCs, numerous approaches and culture protocols have been explored to establish scaffolds<sup>[15]</sup> or niches<sup>[16–18]</sup> that have been equipped with a certain environment for their survival and expansion in ways with high maneuverability.<sup>[19–21]</sup> Currently, mainstream iPSCs cultures are using laminin as a substrate for cell attachment while growing them on the dish.<sup>[22]</sup> However, this substrate is typically 2D in nature

## 1. Introduction


The discovery of the induced pluripotent stem cells (iPSCs) has opened up unprecedented opportunities in the area of clinical therapy, especially for regenerative medicine.<sup>[1–4]</sup> Since iPSCs can be cultured from the patient's cells, transplantation therapies based on these patient-specific cell lines could largely eliminate the immunological rejection<sup>[2–4]</sup> and meanwhile avoid

with a limited ability to recapitulate in vivo-like 3D microenvironment.<sup>[23]</sup> Furthermore, various recent reports suggest that cells cultured on 2D substrates differ greatly from those grown in vivo.<sup>[24]</sup> Additional drawbacks include inherent heterogeneity, limited scalability, and reproducibility.<sup>[13,20]</sup> The most widely used attempt to move cultures from 2D to 3D is to embed cells into Matrigel.<sup>[25]</sup> Matrigel is useful for research purposes, while its semi-chemically defined, xenogeneic substrate property, together with the source of variability and xenogeneic contamination make it incompatible for the generation of clinical grade iPSCs.<sup>[26–29]</sup> Thus developing alternative materials for productive and safe 3D culture environment is strongly desired. Advances in materials chemistry,<sup>[15,21,30–32]</sup> fabricating and processing technologies,<sup>[25,33–36]</sup> and developmental biology<sup>[26,37–39]</sup> have to be coordinately applied in the design of new 3D cell culture matrices that better represent the geometry, chemistry, and signaling environment of the natural extracellular matrix (ECM).

Since ECM is the natural environment for the cell growth and survival, thus, building a 3D microenvironment by mimicking the properties of the ECM is a promising strategy.<sup>[23,38]</sup> Recently, synthetic materials inspired from the construction and role of native ECMs in cell accommodation were produced for the cell culture applications. For example, hydrogels based on biocompatible polymers were produced that incorporated biological cues to define an artificial milieu with complex interactions that regulate

Dr. W. J. Liang, Dr. S. Bhatia, F. Reisbeck, Dr. Y. N. Zhong, Dr. A. K. Singh, Dr. W. Z. Li, Prof. R. Haag  
Institute of Chemistry and Biochemistry  
Free University of Berlin  
Takustr. 3, 14195 Berlin, Germany  
E-mail: wenzhong.li@fu-berlin.de; haag@chemie.fu-berlin.de

Dr. Y. N. Zhong  
Department of Pharmaceutical Engineering  
China Pharmaceutical University  
Nanjing 211198, China

 The ORCID identification number(s) for the author(s) of this article can be found under <https://doi.org/10.1002/adfm.202010630>.

© 2021 The Authors. Advanced Functional Materials published by Wiley-VCH GmbH. This is an open access article under the terms of the Creative Commons Attribution-NonCommercial License, which permits use, distribution and reproduction in any medium, provided the original work is properly cited and is not used for commercial purposes.

DOI: 10.1002/adfm.202010630

and foster stem cells similar to the events occurring in a natural cellular microenvironment.<sup>[40]</sup> For example, Lutolf and coworkers reported adhesion peptide-functionalized enzymatically cross-linked PEG-based hydrogels by chemical gelation for the design of 3D microenvironment to mimic the biochemical features of the native ECMs.<sup>[39]</sup> After modulating micro-environmental stiffness, degradability, and biochemical composition, this synthetic 3D “reprogramming niche” was explored for somatic cell reprogramming and iPSC generation. These synthetic 3D cell culture matrices better represented the geometry, chemistry, and signaling environment of the natural ECM. However, these synthetic 3D systems might not be suitable for the iPSC culture because enzymatic degradation will inevitably be harmful to the proliferated cells. Our group has previously reported a microgel construction kit and successfully realized the pH-controlled release of living cells from the hydrogel by benzacetel bond hydrolysis.<sup>[41]</sup> However, iPSCs are too sensitive to survive acidic pH 6 conditions. Schaffer’s group reported an iPSCs 3D culture system with poly(*N*-isopropylacrylamide)-polyethylene glycol (pNIPAAm-PEG) hydrogels based on a physical thermo-reversible gelation.<sup>[42]</sup> However, physical thermo-reversible materials are usually based on loose gelation strengths, and only under high concentration they can support an iPSCs culture. While under high concentrations, thermo-reversible materials have a strong preference for a defined medium and are even not stable in pure PBS solution.<sup>[43]</sup> Obviously, all of these attempts show some attractive aspects, however, further improvement is still needed to provide an optimal synthetic niche.

In this study, we presented an advanced approach for engineering a synthetic and control-release iPSCs’ 3D artificial niche environment according to a physical–chemical cogelation strategy for iPSCs culture (Figure 1). To achieve this goal, we tailored a 3D microenvironment with two specially designed biocompatible linkers: dendritic polyglycerol-bicyclononyne (dPG-BCN) and poly(*N*-isopropylacrylamide)-*co*-polyethylene glycol azide (pNIPAAm-*co*-PEG-N<sub>3</sub>) polymers in two steps. First, under room temperature, the two polymers could form a hydrogel by strain-promoted azide-alkyne cycloaddition (SPAAC) reaction. After being transferred to culture conditions (37 °C), in which the temperature was higher than the lower critical solution temperature (LCST), the *N*-isopropylacrylamide (NIPAAm)-*co*-polyethylene glycol polymers undergo physical gelation and further form a reversible hydrogel. Under physical-*co*-chemical synergistic gelation conditions, the formed dPG-pNIPAAm-*co*-PEG could mimic the physical property of the ECM. Additionally, rRGD was introduced as biochemical signal to promote cell attachment.<sup>[35,44,45]</sup> After all the foremost parameters about precursor ratios (dPG-BCN [100 mg mL<sup>-1</sup>] and pNIPAAm-*co*-PEG-N<sub>3</sub> [100 mg mL<sup>-1</sup>]), elastic modulus (physical stiffness),<sup>[23,24]</sup> and cell seeding density were optimized, an optimal condition for cell culture was achieved. Therefore, the culture system could support iPSCs’ fast expansion and maintain high quality about proliferation capacity and high pluripotency, which can be characterized by the test of Ki-67 staining,<sup>[46]</sup> alkaline phosphatase (ALP) staining,<sup>[47]</sup> and pluripotency immunostaining.<sup>[1,42,48]</sup> Upon cooling down

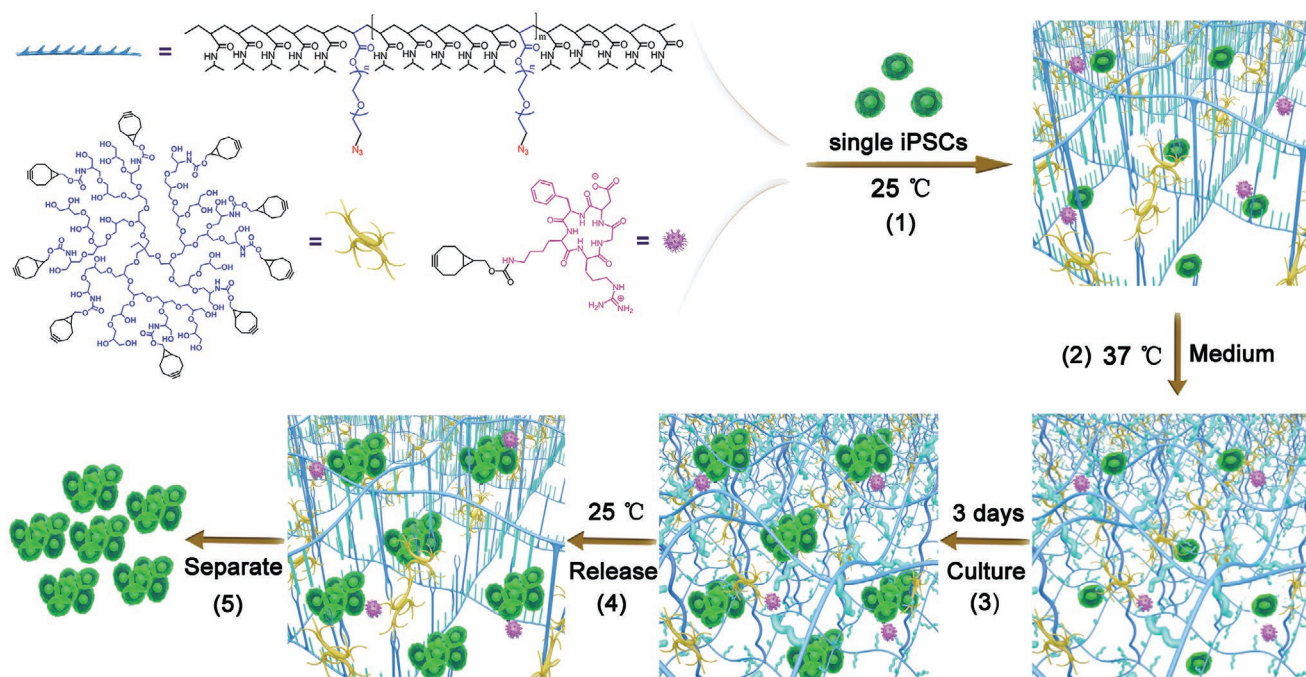


**Figure 1.** Schematic representation of the work mechanism in iPSCs’ 3D culture for the artificial niche built based on dPG and pNIPAAm-*co*-PEG polymers via physical–chemical cogelation strategy: first, a set of synthetic precursors, dPG-cyclooctyne, pNIPAAm-*co*-PEG azide, and RGD-cyclooctyne, was synthesized. 1) Together with these precursors, iPSCs were seeded into the system, and they preliminarily produced a niche only by chemical gelation. 2) After being transferred into 37 °C, physical gelation also occurred and created a reversible hydrogel. 3) Under these conditions, a stable niche was formed by physical–chemical cogelation strategy, which supported iPSCs’ survival and quick expansion. 4) After being cultured for certain time, the system could be transferred to 25 °C again, and the physical gelation disappeared, the niche was loosened, and then the cells released out of the niches. 5) Cells harvest by centrifugation.

to ambient temperature (<LCST), the physical gelation effect disappears leaving alone the covalent bond-based gelation effect. This mechanism precisely benefits the culture system with the ability of controlled release of cells and to harvest them with high yield. Overall, this work provides an advanced control-release hydrogel scaffold with great promise for iPSCs' 3D culture.

## 2. Results and Discussion

### 2.1. Establishment of Control-Release Three-Dimensional Hydrogel-Based Artificial Niche Microenvironment by Extracellular Matrix Mimicking

The native ECM, which works as a key constitutive part of the microniche and plays an essential role in regulating cell behavior, is a complicated system.<sup>[24]</sup> Establishing an artificial niche microenvironment by mimicking the physical and biochemical characteristics of such an ECM, involves the optimization of several parameters, for example, chemically defined cell-compatible material synthesis, hydrogel stiffness, cell seeding density, and adhesion-relative biochemical cues.<sup>[49]</sup> Furthermore, it is crucial to find efficient methods and related vital factors for the design of 3D cell culture niche environment that better represent the geometry, chemistry, and signaling environment suitable for iPSCs' survival and expansion. All optimal parameters and conditions of the above factors and conditions should be coordinated for efficient iPSCs expansion. After these conditions have been modulated, the expanded cells were released under room temperature and the quality of the expanded cells should be further assessed.

#### 2.1.1. Precursors' Synthesis and the Fabrication of Novel Hydrogel Scaffold Niche

For the establishment of a chemically defined niche environment for iPSC culturing, materials that are used to tailor their backbone and supply the cells' physical properties are crucial.<sup>[23,34]</sup> Thus, the design and the specific preparation of the synthetic precursors are the primary steps.<sup>[50]</sup> PEG<sup>[32,51]</sup> and dPG,<sup>[41]</sup> because of their high biocompatibility, low batch-to-batch variability, as well as their readily amenable scalability have shown great promise to act as cellular scaffolds.<sup>[52]</sup> Stimuli-responsive polymer materials are powerful tools in establishing dynamic or control reversible microenvironment, especially in cell biology.<sup>[53]</sup> Among various stimuli triggers, thermoresponsiveness can be easily controlled and is the most promising one to engineer materials for cell loading and release. pNIPAAm has been widely applied as a temperature-sensitive polymer with reversible gelation at the LCST of 32 °C.<sup>[31,54–56]</sup> In order to combine the advantages of both, we synthesized a pNIPAAm-co-PEG polymer, as illustrated in **Figure 2a**. The stimuli-responsive illustration was revealed (**Figure 2b**), and its LCST investigated (**Figure S1**, Supporting Information). After azidation, the pNIPAAm-co-PEG polymer can be applied to program the hybrid hydrogel with dendritic polyglycerol-bicyclooctyne (dPG-BCN) (**Figure 2c**) by the in situ bioorthogonal SPAAC reaction.<sup>[41]</sup> The synthesis and characterization of other macro-monomers and details of their characterization are shown in the Experimental Section. Benefiting from the cogelation strategy, dPG-pNIPAAm-PEG hydrogel networks serve as the backbone of the microniche for supporting cells (**Figure 2e**) better than the pNIPAAm-co-PEG hydrogel networks. On one hand, they overcome the disadvantage caused

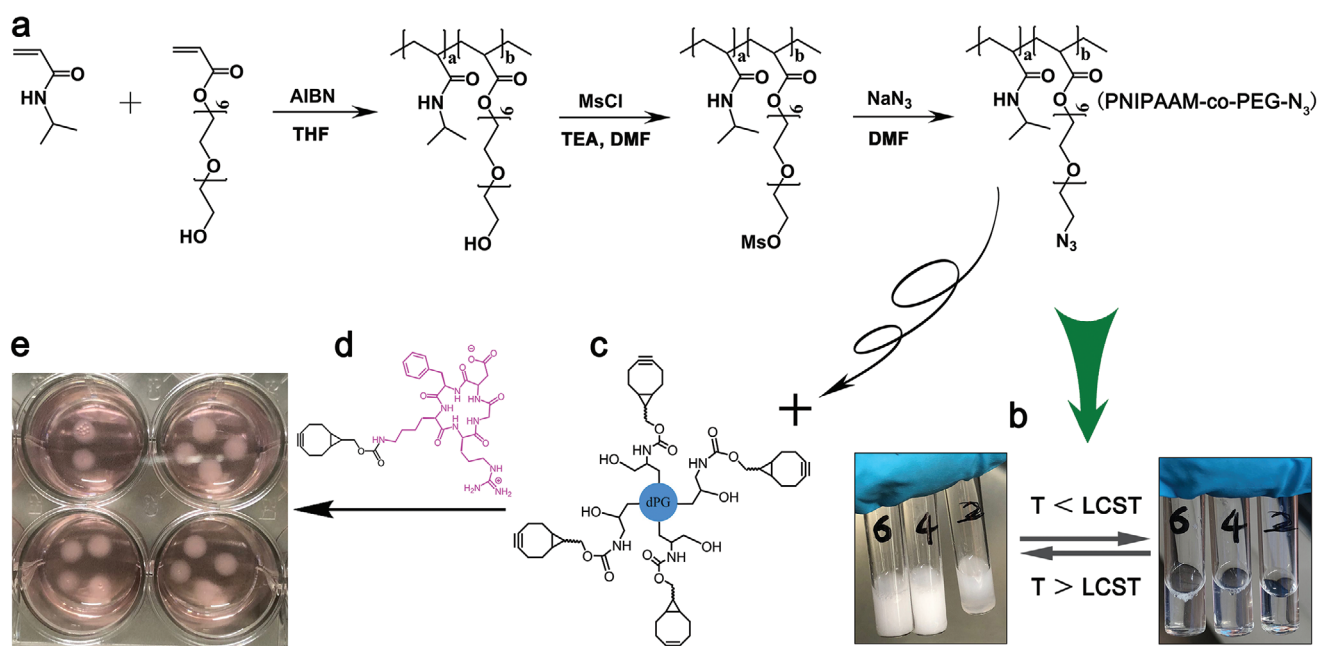


**Figure 2.** Synthesis of the precursors and fabrication process of the hydrogel scaffold's niche: a) Synthesis process of the pNIPAAm-co-PEG-N<sub>3</sub> and its thermo-reversible hydrogel properties. (NiPAAM:PEG-acrylate = 5:1). b) The thermo-reversible phase-change phenomenon of the pNIPAAm-co-PEG-N<sub>3</sub> (LCST ≈ 31 °C). c) dPG-BCN (6%), d) RGD-DIC, and e) the finally formed scaffold niche with iPSCs culture inside under 37 °C (within ESGRO medium).



by a single pNIPAAm-co-PEG polymer, which is that physically cross-linked hydrogels fail to show strength and is not stable enough to serve as a cell scaffold. On the other hand, one must introduce pNIPAAm, which has been equipped with microniche controlled release properties. For stimulating cell adhesion inside the microniche, cyclo (RGDfk), a cellular binding peptide sequence was integrated into the polymer network as a biochemical signal that support iPSCs' survival and proliferation (Figure 2d).<sup>[35,44,45]</sup> Finally, all of these precursors form the thermoresponsive hydrogel microniche (Figure 2e), of which the properties such as elasticity and precursor's contents can be further adjusted.

### 2.1.2. Stiffness Characterization of the Hydrogel Microniche Formed with Various Precursors' Ratios and Concentrations

Substrate stiffness, typically characterized by the elastic modulus, is one of the important mechanical features in controlling cell fate.<sup>[24]</sup> To tailor a microenvironment with proper physical strength, it is essential to optimize the stiffness parameters by adjusting the related factors. Because the hydrogels-based niche was constructed by two precursor polymers, that is, pNIPAAm-co-PEG-N<sub>3</sub> and dPG-BCN, the mechanical stiffness of the hydrogel networks could be regulated by the respective ratios and overall concentration of the precursor. Influence of both of these parameters on the stiffness of the hydrogel networks was studied which led to the establishment of an ideal artificial niche for iPSCs' loading and proliferation (Figure 2). To assess the

effect of precursor ratios, the elastic and viscous moduli were investigated by performing rheological measurements. The ratios of precursors (dPG-BCN to pNIPAAm-co-PEG-N<sub>3</sub>) for gel 1 to gel 6 were accordingly preset as 1:3, 1:2, 2:3, 1:1, 2:1, and 3:1, respectively (Figure 3a,c). Obviously, the elastic and viscous moduli of the hydrogel responded sensitively to the variation of precursor ratios and their data presented a curvilinear distribution. Compared to other gels, gel 3 and gel 4 with content ratio 2:3 and 1:1, respectively, presented a high value of both elastic and viscous modulus. It could be referred from these data that only under certain precursor ratios, the synthesized hydrogel-based microniche environment could be formed with high efficiency and possess an optimal stiffness, especially when the ratio (dPG-BCN and pNIPAAm-co-PEG-N<sub>3</sub>) was 1:1 or 2:3.

Besides the precursor ratios, polymer concentration was another crucial parameter that could affect the stiffness.<sup>[57]</sup> To further investigate the stiffness parameter affected by polymer concentration (Table S1, Supporting Information), a rheological test was performed by varying the polymer concentrations under constant ratio (Figure 3b,d). The rheological curves of all the gels with different concentrations of dPG-BCN and pNIPAAm-co-PEG-N<sub>3</sub> indicated that the strength of the elastic modulus was in accordance with the concentration of the polymer under a specific polymer precursor ratio. Therefore, it is essential to investigate suitable stiffness-related physical parameters for constructing an artificial cell niche. Also, the gelation time, as a crucial parameter to evaluate the gelation efficiency, was essential in determining whether the technique could be used in the niche manufacturing process and

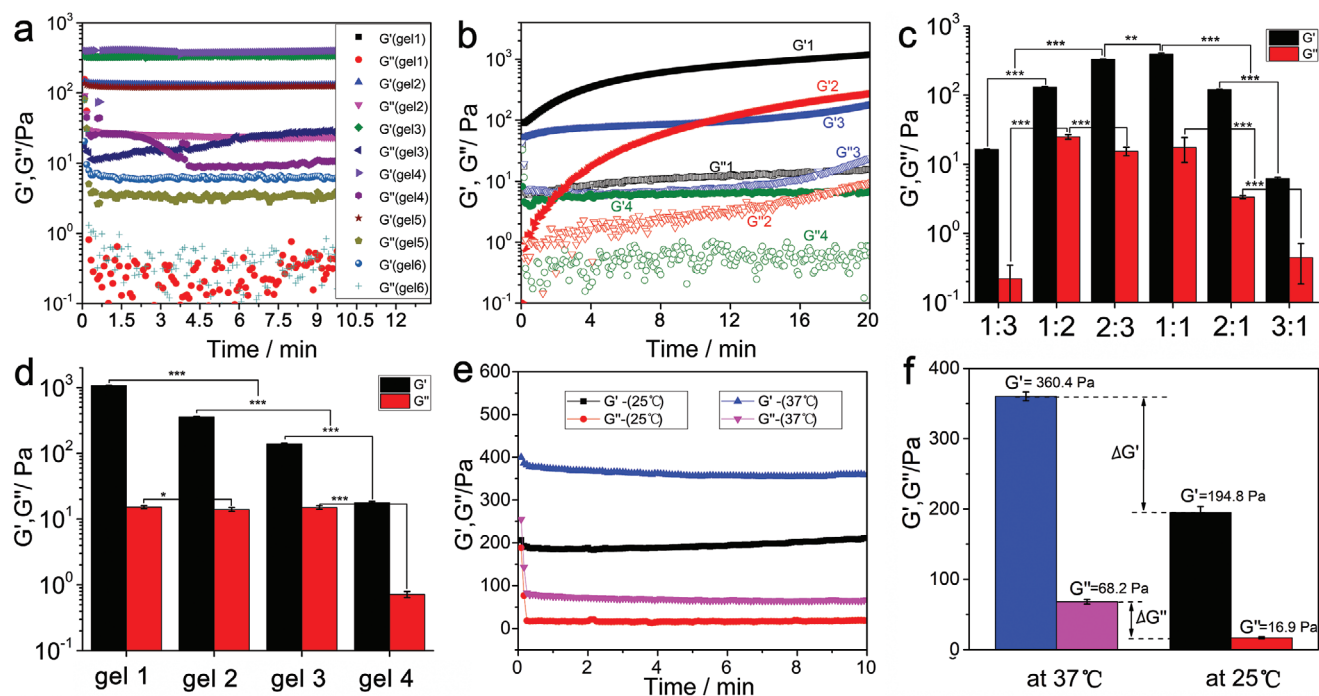


**Figure 3.** a) The elastic modulus,  $G'$ , and viscous modulus,  $G''$ , were tested for the preformed hydrogel with variable volume ratio of dPG-BCN to pNIPAAm-co-PEG-N<sub>3</sub> ( $c_{\text{pNIPAAm-co-PEG-N}_3} = 100 \text{ mg mL}^{-1}$ ,  $c_{\text{dPG-BCN}} = 100 \text{ mg mL}^{-1}$ ) at a constant temperature (37 °C). b) Time-dependent gelation test for system with four different precursor concentrations under a certain ratio (1:1). c) Rheology data of hydrogels niche under various precursor ratios. d) Rheology data of hydrogels niche (gel 1–gel 4) with various precursors' concentrations under certain ratios. e, f) Rheology contribution from different gelation mechanism of hydrogels niche under different temperature. \* $p < 0.05$ , \*\* $p < 0.01$ , and \*\*\* $p < 0.001$ .



supplied us with an appropriate incubation time during the initial period of cell seeding and cultivation. Thus, from the time-dependent elastic modulus,  $G'$ , and viscous modulus,  $G''$ , test, the effect and relationship of temperature and gelation time were also investigated during the gelation process. As shown in Figure 3b, gelation time was, respectively, about 20 min under the temperature of 37 °C. In consideration of the operation and 3D scaffold niche manufacture process, 20 min was the best choice for the parameters of gelation time for this application. On the whole, these results demonstrated that the mechanical properties of the gel were governed by a complex interplay of dPG-BCN and pNIPAAm-co-PEG- $N_3$ . It could be regulated by modulating the ratios and content of these polymers.

### 2.1.3. Induced Pluripotent Stem Cells' Response to the Precursors Ratios of Materials for Establishing a Three-Dimensional Niche Environment

For a holistic study of the artificial 3D niche environment design, pivotal parameters should be coordinated and controlled to render a suitable microenvironment that can affect cellular responses. In spite of the dPG-BCN and

pNIPAAm-co-PEG- $N_3$  exhibiting good gelling mechanical strength by modulating their ratios, it is still unclear how the iPSCs respond to the extracellular niche environment resembled by precursors with different ratios. Due to the precursor ratios that would determine the hydrogel composition and topography, we performed the artificial extracellular niche's interior morphology analysis (Figure 4a). The results revealed that the precursor ratios have a deep influence on the interior niche structure and determine the size, density, as well as the order of the porosity inside the networks. To assess whether the different ratios of precursors affect iPSCs' survival and proliferation, iPSCs were further embedded into hydrogels precursors with six different ratios ( $R_1$ – $R_6$ ) and cultured in an incubator under 37 °C. During the culture process, the cell survival and morphology features were monitored by live/dead staining. The investigations' results (Figure 4b) indicated that the ratio of precursors could readily affect the behavior of the cells inside the niche. In a niche environment with precursor ratio of  $R_1$  (dPG-BCN:pNIPAAm-co-PEG- $N_3 = 1:3$ ,  $E \approx 16$  Pa), only very few cells survived and aggregated. After three days of culture (day 3), there were obviously dead cells on the surface on the cell agglomeration. Until day 5, cell agglomeration occurred and formed embryoid bodies (EB) with a large size (more than

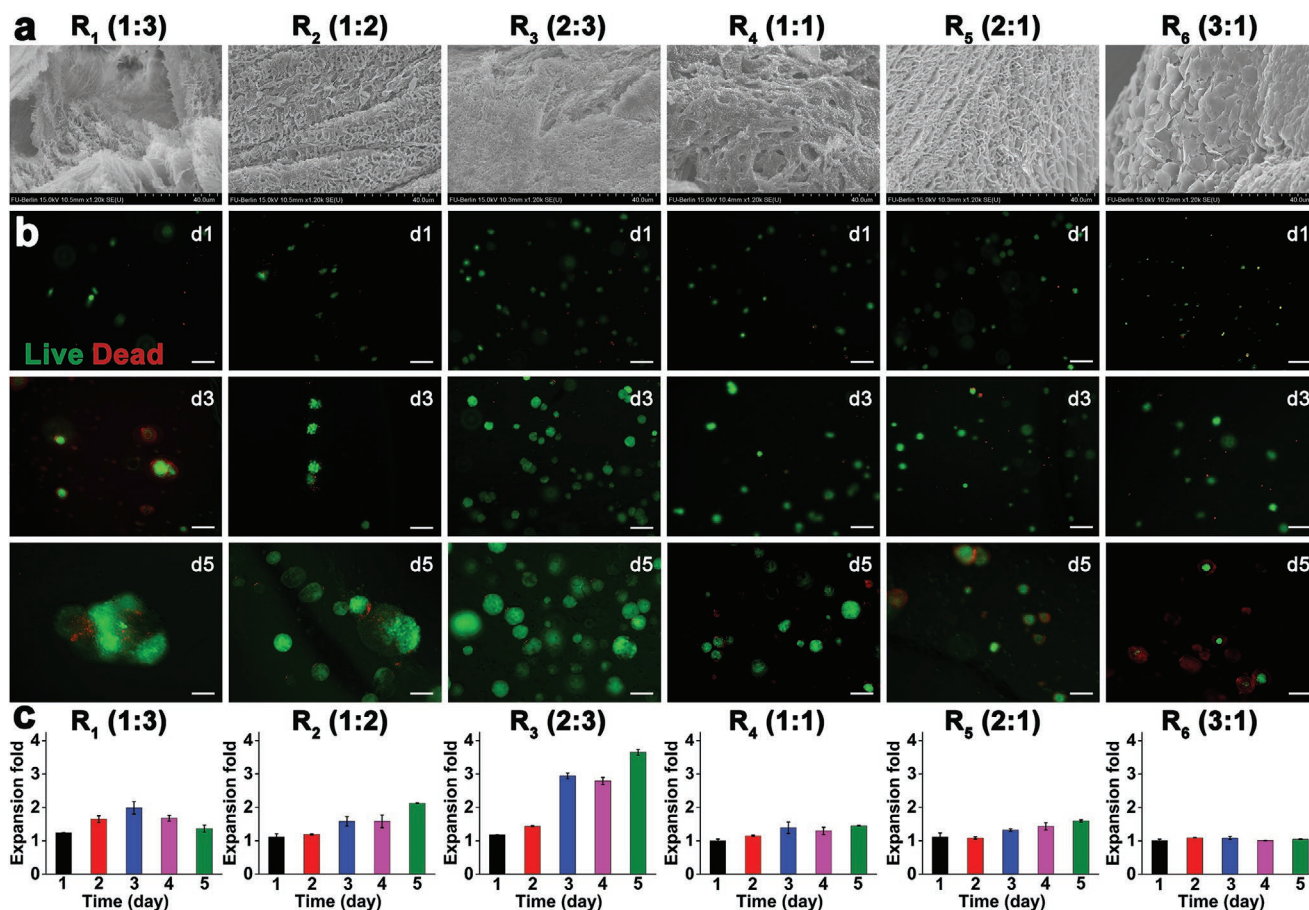


**Figure 4.** The response of iPSCs' viability and scaffold environment morphology to precursor ratios of the hydrogels niche. a) SEM morphology test response to the precursor ratios of the hydrogel niche. The scale bar indicates 40  $\mu$ m. b) Cell viability tests depending on the precursor ratios of the hydrogel niche was monitored by live/dead staining (green = live cells, red = dead cells). The scale bar indicates 100  $\mu$ m. c) The iPSCs' proliferation as performance response to the precursor ratio of the hydrogel.

300  $\mu\text{m}$ ). The fact revealed that a microniche environment with precursor ratio  $R_1$  could not support iPSCs' culture. These phenomena can be explained by the fact that, under this precursor ratio (3:1), the content of dPG-BCN is much lower than that of pNIPAAm-co-PEG- $\text{N}_3$ , which would predominantly lead to physical gelation rather than chemical SPAAC gelation within the cogelation system. It additionally also indicated that, with peristalsis phenomena, the physical gelling of pNIPAAm gel could not supply enough strength to prevent cell agglomeration, especially in the scaffold formed with pure or too much pNIPAAm physical gelation. Compared to the situation of  $R_1$ , cells in niche environment with the precursor ratio of  $R_2$  (dPG-BCN:pNIPAAm-co-PEG- $\text{N}_3 = 1:2$ ,  $E \approx 120$  Pa) and  $R_3$  (dPG-BCN:pNIPAAm-co-PEG- $\text{N}_3 = 2:3$ ,  $E \approx 330$  Pa) survived better. Especially under  $R_3$ , culturing cells in a niche environment formed dense, uniform, and small spheroids with high cell viability. This showed that the hydrogel niche with the current precursor ratio could better support iPSCs' survival. It also revealed that, under a certain ratio (2:3), coordination and balance of the chemical and physical gelation could be achieved to prevent cell agglomeration, which supports iPSCs' survival and expansion. While the situation of  $R_4$ ,  $R_5$ , and  $R_6$ , with the content increase of dPG-BCN and the content decrease of pNIPAAm-co-PEG- $\text{N}_3$ , benefitted from the adequate SPAAC reaction and chemical covalent gelation, the niche environment could still prevent cell agglomeration. However, they could not support the cells to simultaneously keep high viability as well, because the low degradability of their network would limit the cells' growth. Besides, the expansion test (Figure 4c), of which the significant difference was labeled in Figure S2, Supporting Information, further revealed that a niche with a precursor ratio of 2:3 shows the best performance for iPSCs' survival and expansion. Especially, after 3 days, the niche environment with these precursor ratios could better maintain iPSCs' renewability and has a higher expansion rate. So, the precursor ratio of 2:3 (dPG-BCN:pNIPAAm-co-PEG- $\text{N}_3$ ) could be regarded as the best ratio to form the niche environment for iPSC culturing. Hence, we selected this composition of the gel as a standard for further studies during the following experiments.

#### 2.1.4. Induced Pluripotent Stem Cells' Viability to the Stiffness and Precursor Content of the Three-Dimensional Niche Environments

Previous studies reported that signals from the extracellular environment, especially the mechanical feedback of the linkage between cell and substrate, play a key role in regulating stem-cell fate.<sup>[58]</sup> The extracellular environment varies not only in composition but also in physical parameters, including stiffness, which typically is characterized by the elastic modulus and topography.<sup>[59]</sup> So, it is essential to investigate how the cells are influenced by the topography and stiffness in our artificial niche environment. Control of the polymer concentration or cross-linking density varies topography and hydrogel stiffness.<sup>[23]</sup> Therefore, morphological properties of the niche environment with various polymers were adapted to test how their morphology was affected by the cross-linking density. Alterations in the concentration ratio of various polymers influenced the cell fate (Figure 5). The morphology analysis (Figure 5a) of

concentrations should be studied first. However, as mentioned above, the precursor ratios also showed a particular effect in determining the stiffness of the niche environment. To circumvent the stiffness change caused by ratio variation, all the niche environment was performed by scanning electron microscopy (SEM), the results revealed that the inside niche environment took on a porous cellular structure. Whereas, in all of the niche environments with different stiffness the morphology around holes varied according to elastic modules. In a slightly less cross-linked gel ( $E_3 \approx 139$  Pa) and  $E_4 \approx 178$  Pa), the size of the hole was a little larger. While, conversely, in slightly more cross-linked gels ( $E_1 \approx 1070$  Pa) and  $E_2 \approx 357$  Pa), the size of the hole was a little smaller. This study demonstrates that the size of the hole is closely related with the gel stiffness, which is determined by the precursor concentrations (Table S1, Supporting Information) that were used to construct the polymeric gels.

In order to assess whether the different stiffness of the niche scaffold affected iPSCs' survival and proliferation, iPSCs were embedded into hydrogels precursors with high, medium, low, and really low concentrations, respectively, of which the elastic moduli ranged from 1070–178 Pa accordingly (Figure 5). Meanwhile, cells were cultured in the ESGRO medium, and their survival conditions were monitored at least for 3 days (Figure 5b). The results revealed that cell behavior in this artificial niche was significantly affected by the stiffness of their microenvironment. First, cells can form dense, uniform spheroids under all stiffness parameters at the beginning, which demonstrates the biocompatibility of these materials. However, specific stiffness is essential to prevent cells from agglomerating. Without enough stiffness, the microenvironment was insufficient to support the cell spheroids—EB, such as situations that occurred in  $E_3$  (139 Pa) and  $E_4$  (178 Pa), and these EB would aggregate with each other and form supersize agglomerations. This was further demonstrated in the cell expansion test (Figure 5d). In the low stiffness niche environment, almost no cell expansion occurred. Compared to these, culturing cells in the niche with medium stiffness, uniform spheroids could form quickly and these iPSCs proliferated fast. The average size of the EB could reach 44.8  $\mu\text{m}$  (day 3) from 24  $\mu\text{m}$  (day1) (Figure 5c), and the expansion rate could reach 6.5-fold (day 4) from 3.5-fold (day 4) (Figure 5d). While under high stiffness environment  $E_1$  (1075 Pa), most iPSCs have a lower cell survival rate and relatively poor expansion efficiency. Both the size and the number of the EB were much lower than that in medium stiffness environment (Figure 5c). This was also revealed from the expansion test (2.3- and 3.3-fold for day 1 and day 3, respectively) (Figure 5d), of which the significant difference was labeled in Figure S3, Supporting Information. Overall, this study revealed that only a certain stiffness environment allows for iPSCs' survival and expansion well. Therefore, the elastic modulus of 357 Pa was chosen as the standard stiffness parameters for the dPG-pNIPAAm-co-PEG-based 3D niche environment culture system.

#### 2.1.5. Induced Pluripotent Stem Cells' Viability and Expansion Efficiency with Regard to Cell Seeding Density

In the extracellular environment, cells do not live alone. They can secrete substances that affect surrounding cells and keep



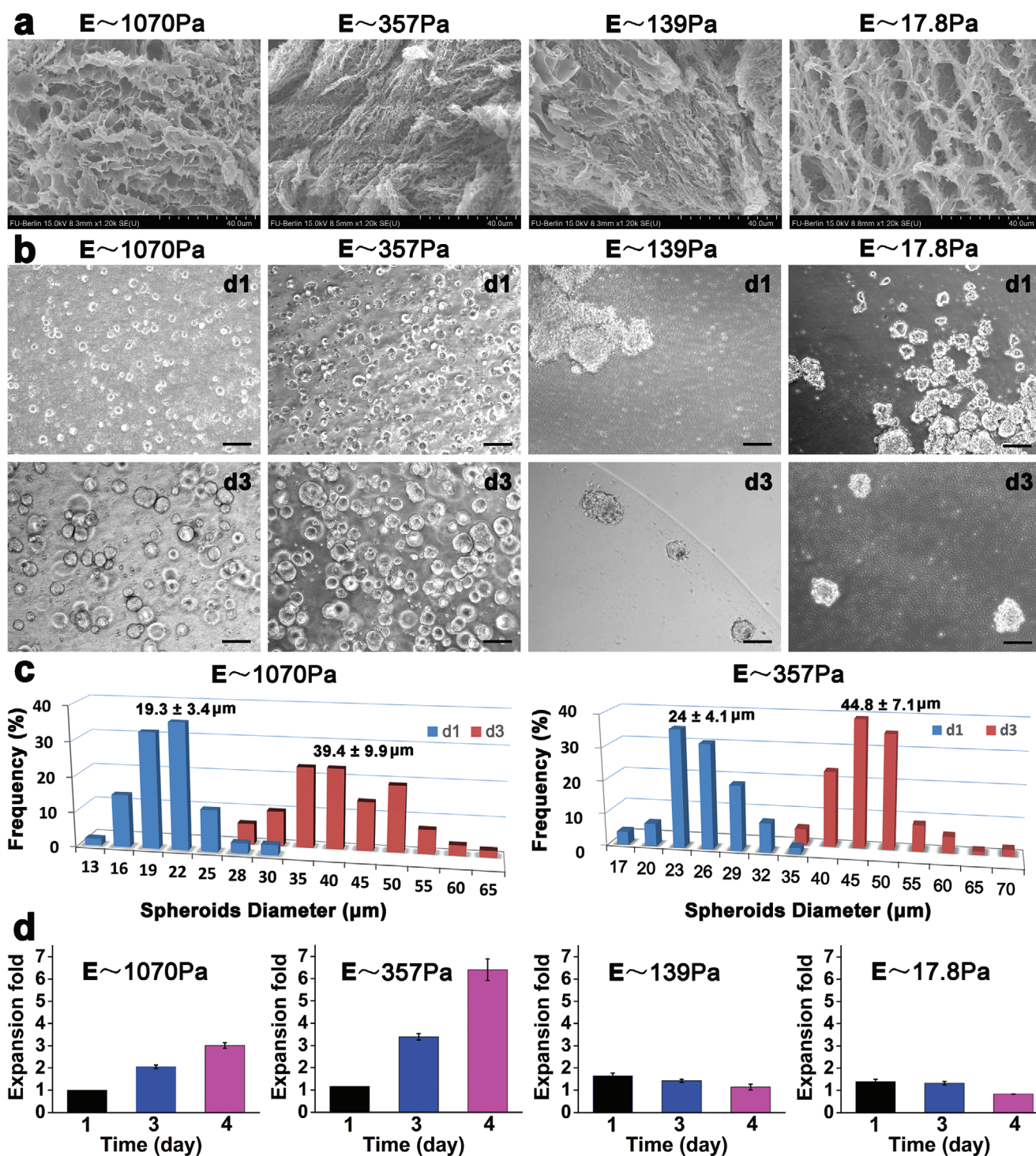


**Figure 5.** The iPSCs' viability and artificial niche environment's morphology in response to the stiffness and precursor content of the hydrogels. a) SEM morphology in response to the stiffness and precursor content of the hydrogels niche (with elastic modulus of 1070, 357, 139, and 17.8 Pa, accordingly). The scale bar indicates 40  $\mu\text{m}$ . b) Cell viability in response to the stiffness and precursor content of the hydrogels niche were monitored by bright field microscopy. The scale bar indicates 100  $\mu\text{m}$ . c) EB size distribution and frequency in different culture days. d) The iPSCs' proliferation efficiency in response to the stiffness of the hydrogel niche environment.

sensing with each other.<sup>[24,59]</sup> Thus, cell distribution and seeding density work as crucial determiners that not only affect the cell-cell contact but also affect cells' survival and

expansion in the artificial niche environment. To further investigate the relationship between the iPSCs' seeding density and expansion efficiency in this prepared niche environment and



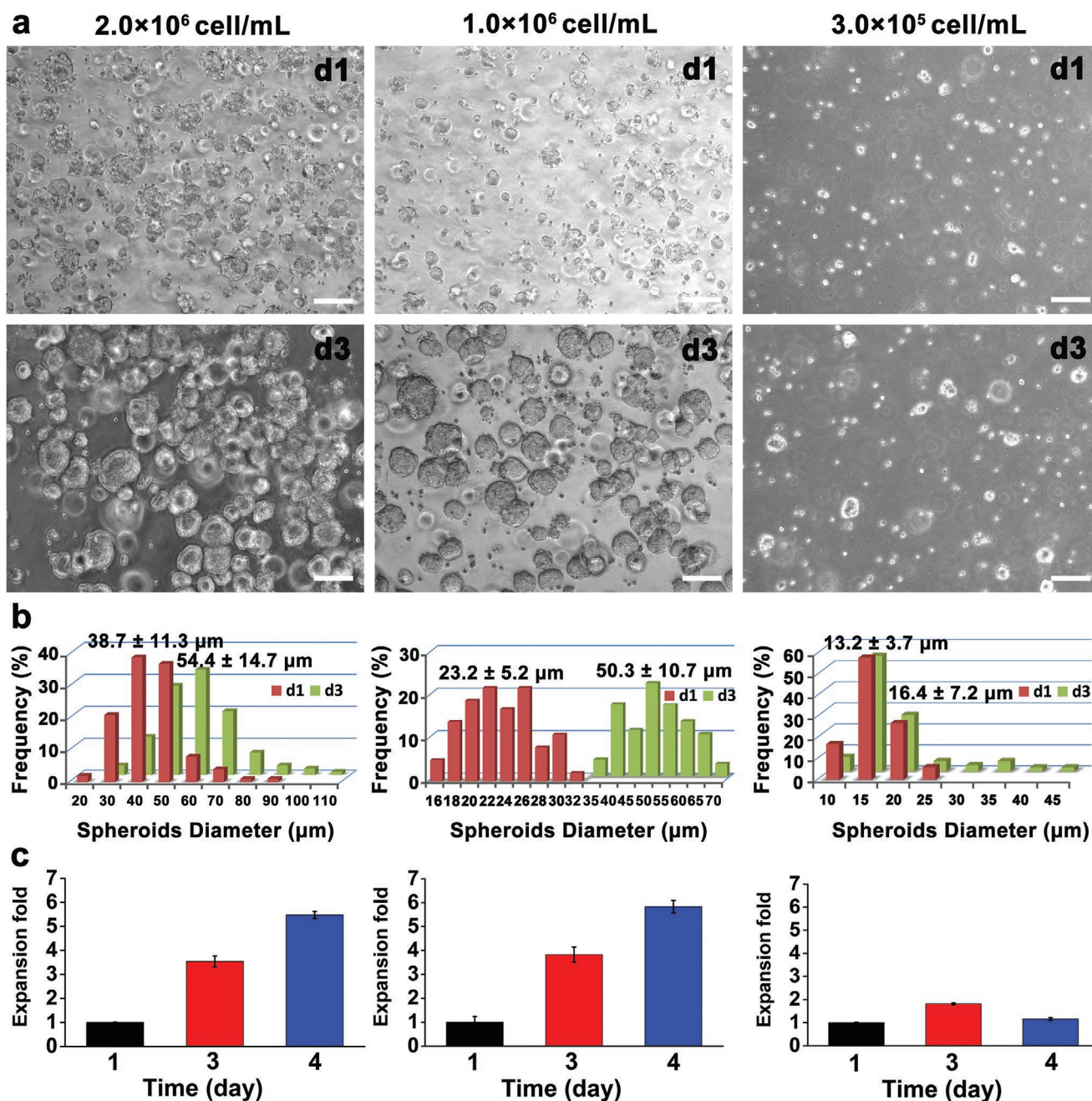


**Figure 6.** Optimization of the cell seeding density for iPSCs expansion in dPG-pNIPAAm-co-PEG niche 3D culture system (scale bar = 100  $\mu\text{m}$ ). a) Cell viability test of the cell seeding density was monitored by bright field microscope. b) EB size distribution and frequency in different culture days to cell seeding density. c) The iPSCs' proliferation efficiency response to culture time under different cell seeding densities in the artificial niche environment.

finally determine the optimum seeding density, cells with different (high, medium, low) concentrations of  $2 \times 10^6$ ,  $1 \times 10^6$ ,  $3 \times 10^5$  cells/mL were separately seeded in three scaffold niches with the same elastic modulus (357 Pa) and specific precursor ratios (dPG-BCN:pNIPAAm-co-PEG- $\text{N}_3$  = 2:3). Furthermore, the morphology of the cells that survived in the artificial niche environment was monitored (Figure 6a). Remarkably, under high or medium seeding density, the cells cultured grew very fast and formed EB soon, while, under low seeding density, the cells expanded and grew into spheroids slowly. According to

the statistical analysis, EB formed in the niche microenvironment with medium seeding density showed a much narrower size distribution than those under low and high seeding density conditions (Figure 6b). During day 1, the average EB sizes for high, medium, and low seeding density were 38.7, 23.2, and 13.2  $\mu\text{m}$ , respectively. While, until day 3, average EB sizes for high, medium, and low seeding density niche environments reached 54.4, 50.3, and 16.4  $\mu\text{m}$ , respectively. The expansion rates of iPSCs in niche with seeding density of  $1 \times 10^6$  cells/mL was 3.82- and 5.83-fold at day 3 and day 4, respectively

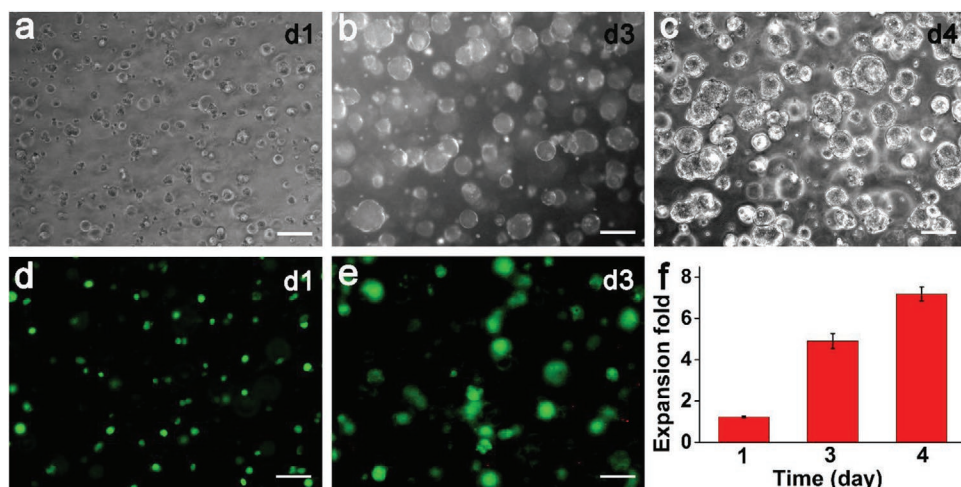


**Figure 7.** The dPG-pNIPAAm-co-PEG niche scaffold-based 3D culture system support iPSCs' expansion well under optimized conditions (scale bar = 100  $\mu\text{m}$ ). a–c) Cell viability and morphology during the culture process at days 1, 3, and 4, respectively. d,e) Cell viability test at days 1 and 3 was monitored by live/dead staining (green = live cells, red = dead cells). f) iPSCs' proliferation efficiency under optimal conditions.

(Figure 6c, of which the significant difference was labeled in Figure S4, Supporting Information), and was higher than those with seeding densities of  $2 \times 10^6$  cells/mL (3.54- and 5.47-fold at day 3 and day 4, respectively) and  $3 \times 10^5$  cells/mL (1.82- and 1.16-fold at day 3 and day 4, respectively).

Additionally, EB size distribution in niche with medium seeding density was 16–32  $\mu\text{m}$  on day 1 and 35–70  $\mu\text{m}$  on day 3, which were much narrower than those in niche with high seeding density (20–90  $\mu\text{m}$  on day 1 and 30–110  $\mu\text{m}$  on day 3) or low seeding density (10–25  $\mu\text{m}$  on day 1 and 10–45  $\mu\text{m}$  on day 3) (Figure 6b). Hence, high seeding density caused the formed EB to aggregate and might limit their rapid expansion, and a low seeding concentration might slow down the EB formation, thus reducing the cell expansion efficiency in this 3D microenvironment. Overall, considering all the above factors, a seeding concentration of  $1 \times 10^6$  cells/mL can be chosen as the most reasonable seeding density for the iPSCs expansion in our niche culture system.

### 2.1.6. Overall Performance of dPG-pNIPAAm-co-PEG 3D Niche Culture System in Supporting Induced Pluripotent Stem Cells' Proliferation

As reported, *in vivo* cells reside in a complex “microniche” environment. This microenvironment generally not only serves as a structural support for cells but also offers various biochemical cues that regulate cell behavior.<sup>[24]</sup> Among these cues, the cell's adhesion site is essential in determining cells viability and proliferation. To stimulate cell adhesion inside the microniche, cyclo (-RGDfK), a cellular binding peptide sequence, was integrated into the polymer network as a biochemical signaling agent.<sup>[44,45]</sup> The concentration of the cyclo (-RGDfK) was adjusted to 1 mM, which was reported as the common reasonable concentration.<sup>[60]</sup> We embedded iPSCs ( $1 \times 10^6$  cells/mL) with precursors (dPG-BCN and pNIPAAm-co-PEG- $\text{N}_3$ , both of their concentration were 100 mg mL<sup>-1</sup>, the ratio of them was 2:3, cyclo (RGDfK) 1mM) into the culture system ( $E_2 \approx 357$  Pa),

to investigate the cell viability and expansion efficiency and overall to assess the performance of the artificial 3D niche environment in iPSCs' culture (Figure 7). Under optimal conditions, single iPSCs cultured in the 3D microenvironment (with RGDSK culture medium) grew very fast and soon grew into dense, uniform, and small spheroids. Then, these spheroids expanded quickly and took on narrow size distribution (Figure 7a–c). Furthermore, the live/dead staining test indicated that cells cultured in this artificial environment had a high viability. Almost all cells kept their renewal ability (Figure 7d,e). This was also demonstrated by the expansion test (Figure 7f). Under optimal conditions, the expansion rates of iPSCs in our niche culture system can achieve efficiency as high as 4.9- and 7.18-fold at day 3 and day 4, respectively. The study revealed that the dPG-pNIPAAm-co-PEG niche 3D culture system could allow for the robust proliferation of iPSCs with high viability. To investigate whether the dPG-pNIPAAm-co-PEG niche has a strong preference for specific medium, the dPG-pNIPAAm-co-PEG niche was also formed in both E8 and ESGRO medium, respectively, and we found the dPG-pNIPAAm-co-PEG materials performed well in both media tested. Overall, the cogelation of dPG-pNIPAAm-co-PEG-based culture system with optimal parameters could support iPSCs proliferation with excellent expansion efficiency without the limitation of a specific medium.

### 2.2. Controlled Release and Cell Harvest

Hydrogels represent an essential class of biomaterials for applications in 3D cell culture because their mechanical properties are similar to those of many objects in a living system.<sup>[40,41]</sup> However, in spite of availability of supplying high biocompatibility, low batch-to-batch variability, facile mechanical tunability, amenable large-scale manufacturing, and showing a great promise in acting as 3D cell-culturing scaffolds, the selective degradation of hydrogel scaffold and how to release the expanded cells with precise control and appropriate rate is



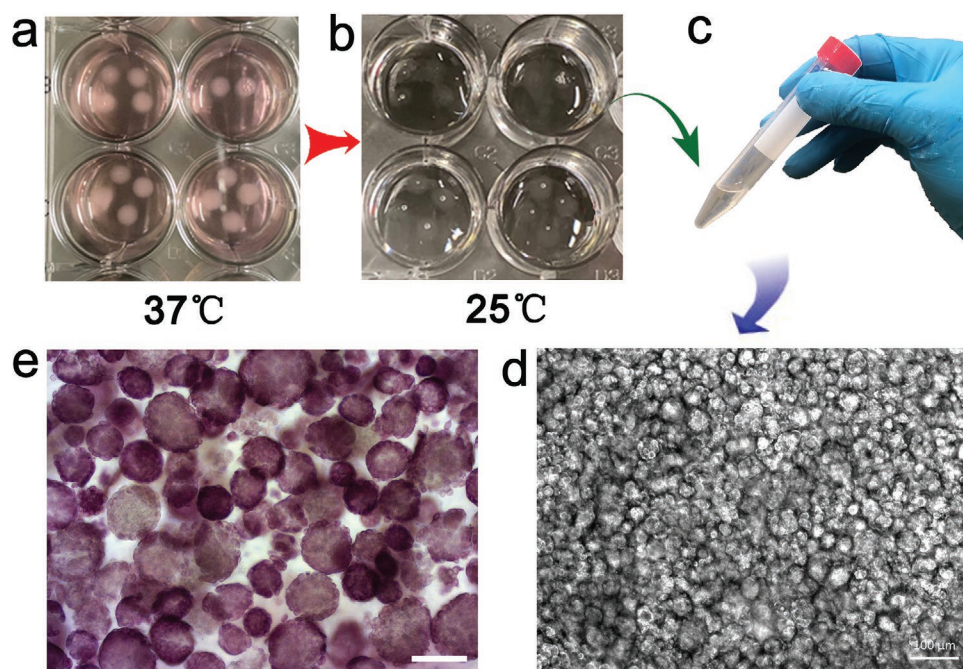


**Figure 8.** Controlled release and harvest of the expanded iPSCs from the dPG-pNIPAAm-co-PEG cogelation niche culture system. a) iPSCs were mixed with precursors and embedded into the culture system and cultured for some time. b) Culture medium was replaced by the PBS, and the culture dish was incubated at 25 °C (<LCST) for 5 min to release the expanded cells. c) iPSCs EB purification and collection by centrifugation. d) EB cells were cultured for 3 days (scale bar = 100 μm). e) Alkaline phosphatase (ALP) staining (scale bar = 50 μm).

still a crucial challenge in these applications.<sup>[61]</sup> To achieve of hydrogel degradation, different strategies for cleaving chemical bonds in the hydrogels networks have been applied. For example, photolytic,<sup>[62]</sup> hydrolytic,<sup>[63]</sup> enzymatic degradation,<sup>[35]</sup> and hydrolysis under acidic pH<sup>[63]</sup> have a great potential for degradation mechanisms which have been tried for controlled release applications.<sup>[42]</sup> However, for these strategies, the photo energy, the hydrolytic initiator, enzyme, and the acidic pH environment would inevitably damage the viability of the cells and might also lead to cell differentiation. To circumvent such a delicate problem, we introduced a release property by the mechanism of thermo-reversible gelation into covalent cross-linking gelation and formed a physical and chemical cogelation system. In this way, the cogelation degree of the niche scaffold could be adjusted by temperature (LCST), which could be used as a strategy to achieve controlled release of the iPSCs from their culture system (**Figure 8**). In this work, iPSCs were first mixed with precursors and embedded in the niche scaffold culture system during the gelation process. After that, they were cultured for 3 days in cell incubator (37 °C) (**Figure 8a**). To release the expanded cells, the culture medium was replaced by the PBS, and the culture dish was incubated at 25 °C (<LCST) for 5 min. During this process, due to the reversibility of the physical gelation process, the thermo-gelation disappeared, leaving behind a loose network of covalently cross-linked gel (**Figure 8b**). After the morphology of the niche scaffold changed from white turbid solid to transparent and colorless, cells and niche scaffold were together transferred into a centrifuge tube (**Figure 8c**). By centrifugation, released iPSCs' EB that were formed in the niche environment were separated, collected, and finally reached cell harvest (**Figure 8d**). According to the

preliminary proliferation test, continuous high expressions of ALP were detected during the culture period until the 7th day (**Figure 8e**). This revealed that iPSCs' EB harvested from our culture system still maintained their proliferation ability well. Besides, the release efficiency for cells after five passages culture had also been discussed (**Figure S6**, Supporting Information). This study showed that the chemically defined dPG-pNIPAAm-co-PEG cogelation niche scaffold culture system not only offers many features that benefit iPSC cultures, such as supporting cells' rapid growth and prevention of forming large cell aggregates, but also supplies thermo-reversible degradation and thus enabling a controlled release of the expanded cells from their culture system. Moreover, the controlled release can be achieved by only adjusting the temperatures, which allows substantial convenience and maneuverability.

### 2.2.1. Cell Quality Characterization

To further assess the performance of the chemically defined dPG-pNIPAAm-co-PEG cogelation niche scaffold culture system, we performed Ki-67 staining test (**Figure 9**) and the immunocytochemistry analysis of pluripotency markers (**Figure 10a**) to investigate their proliferation ability and whether iPSCs could maintain pluripotency throughout the entire culturing process. First, investigations of Ki-67 staining from day 1 to day 5 showed that iPSCs in the spheroids maintained a high expression of Ki-67 proliferation markers. This means that the dPG-pNIPAAm-co-PEG cogelation niche scaffold culture system could support the expanded cells to keep high proliferation ability. Beyond that, immune-fluorescent



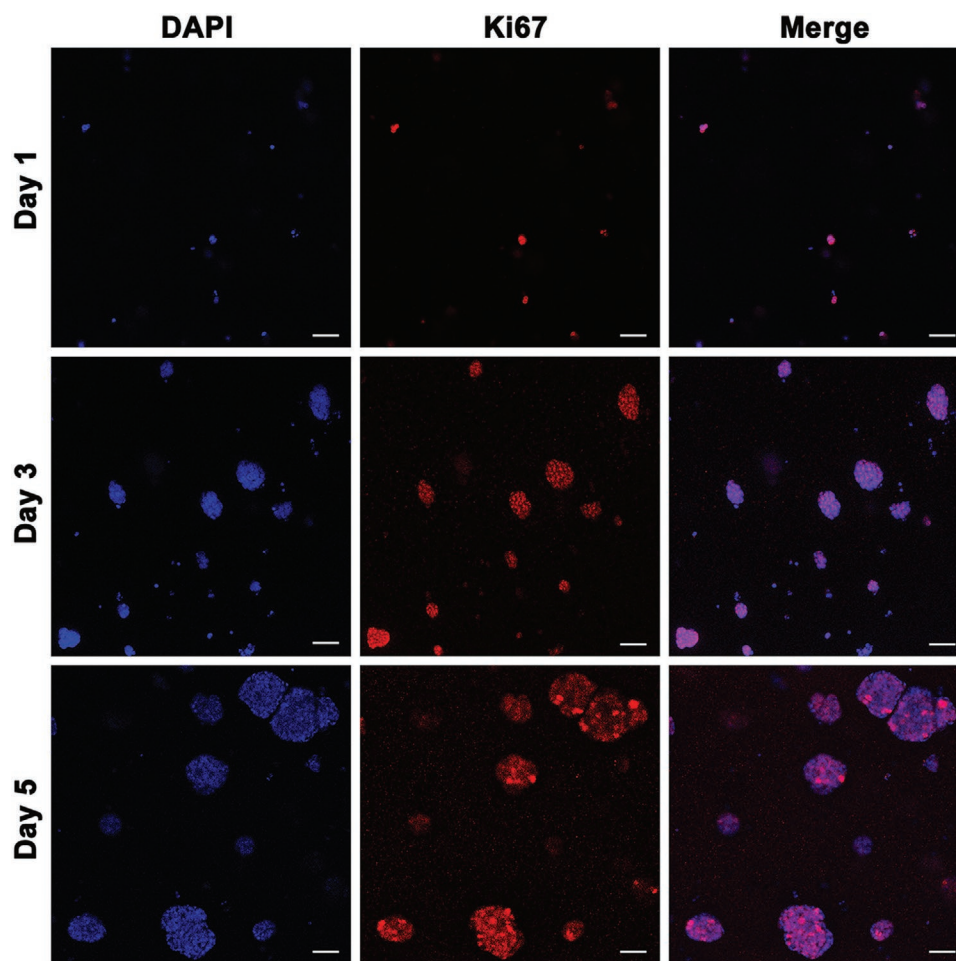


**Figure 9.** Ki-67 staining of the iPSCs' EB after having been cultured for 1, 3, and 5 days, respectively. (Blue: DAPI, red: a marker of proliferating cells) (scale bar = 100  $\mu\text{m}$ ).

staining revealed that the chemically defined cogelation 3D niche-produced iPSCs in spheroids maintained high expression of pluripotent markers,<sup>[1,17]</sup> including Nanog, Sox2, Oct4, and SSEA1 (Figure 10a). In summary, together with the consistent cell growth and ALP staining (Figure 8d), the uniform expression of these proliferation and pluripotent markers deeply revealed that the current system highly expanded iPSCs with high quality, density, and efficiency. Overall, our approach demonstrated that this chemically defined dPG-pNIPAAm-co-PEG cogelation microniche scaffold culture system 3D supported iPSCs' proliferation and expansion well.

Generally, 5 days is relative short time and maybe not long enough to investigate pluripotency maintenance for any culture platform. Typically, at least five passages are required to sufficiently assess pluripotency maintenance. Therefore, for the cells that got from the harvest after 3 days' culture (Figure 8d), we trypsin-dispersed them into individual cells and cultured for another five passages. Then, the fifth passage cells were characterized by immunostaining the pluripotent markers of Nanog, Sox2, Oct4, and SSEA1 again after they had been cultured for 1, 3, and 5 days separately (Figure 10b). The uniform expression of these pluripotent markers deeply revealed that the current system can still expand iPSCs with high quality performance at

least even for five passages. Additionally, in case the pluripotent marker expression is not sufficient to indicate pluripotency, we need to further investigate their pluripotency maintenance in a more standard way. The gold standard for investigating pluripotency maintenance is EB differentiation into the three germ layers test. Thus, to sufficiently assess pluripotency maintenance, we have cultured the cells five passages and made the fifth passage cells characterized by EB differentiation test. As shown in **Figure 11**, immunostaining detected cells positive for  $\alpha$ -smooth muscle actin (mesoderm marker), FOXA2 (endoderm marker), and  $\beta$  III tubulin (ectoderm marker), which means that, after being cultured for five passages, the iPSCs could differentiate into all three germ layers in vitro. These experiments demonstrated that the current system produced-iPSCs in deed keep high pluripotency maintenance.

### 3. Conclusion

In summary, we developed a thermoresponsive hydrogel for the controlled release of iPSCs based on dPG and pNIPAAm-co-PEG polymers via physical-chemical-cogelation. This chemically defined microniche environment supported the robust

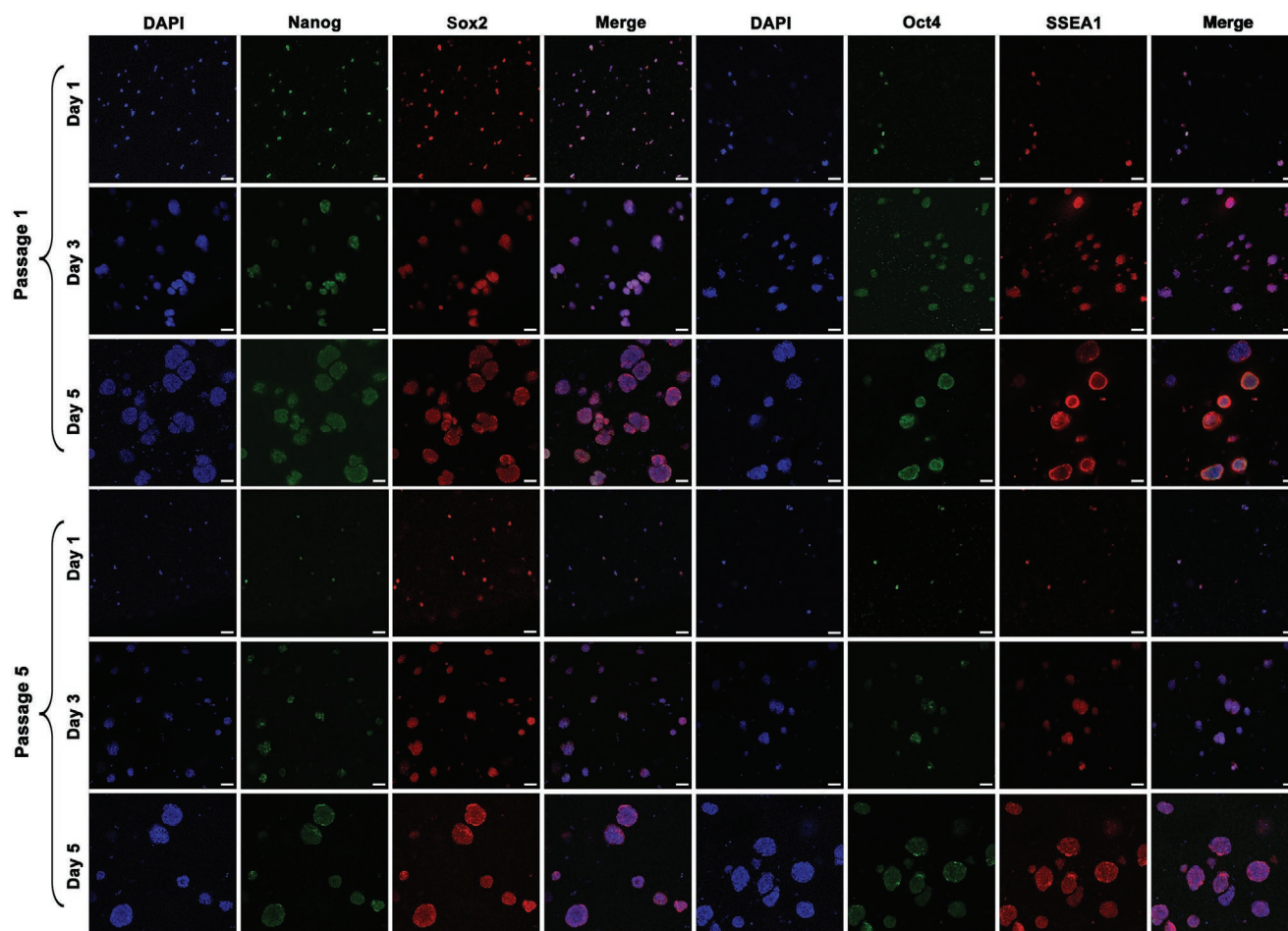


**Figure 10.** Immunostaining of the spheroids shows that the cells expressing the pluripotent markers of Nanog, Sox2, Oct4, and SSEA1. a) All the staining tests were performed after the iPSCs' EB were cultured for 1, 3, and 5 days, respectively. b) After been cultured for five passages, the cells were investigated again by performing the immunostaining staining tests again. In both (a) and (b), scale bar indicates 100  $\mu\text{m}$ .

production of iPSCs with strong maintenance of pluripotency and self-renewal ability. Their expansion efficiency could reach as high as 4.9- and 72-fold within only 3 and 4 days' culture, respectively. Due to the fully chemically defined properties, this 3D culture system could supply iPSCs without any reproduction limits and risks for pathogen and immunogenic transfer

that might be caused by the application of traditional poorly defined animal-derived matrices or cell derivatives. Therefore, it exhibits a great promise for iPSCs to keep their full potential in downstream biomedical applications. Furthermore, our system obtained from the optimized physical-chemical-cogelation strategy substantially overcomes the strong preference for

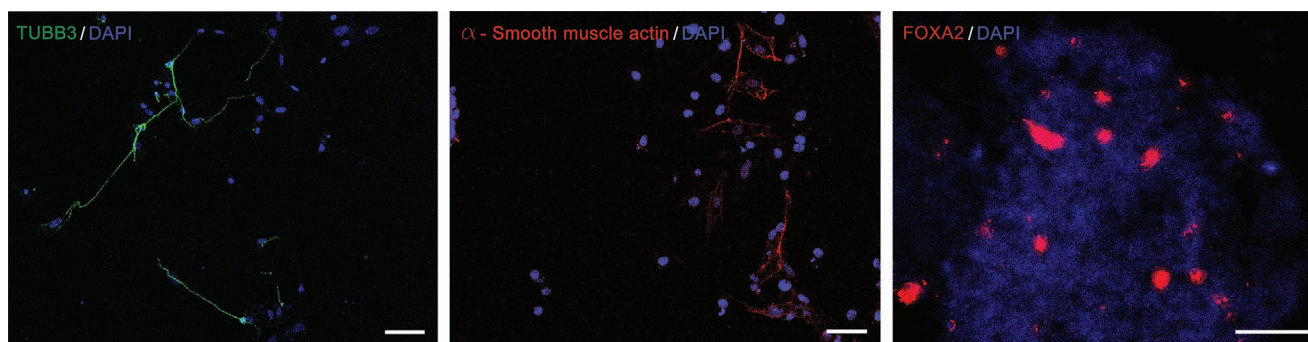


**Figure 11.** a–c) Immunostaining confirming in vitro differentiation of iPSCs into all three germ layers: neuroectodermal (TUBB3), mesodermal ( $\alpha$ -Smooth muscle actin), and endodermal (FOXA2) cell types. Scale bars in (a) and (b) indicate 50  $\mu\text{m}$ , scale bar in (c) indicates 100  $\mu\text{m}$ . Secondary antibodies were labeled with Alexa 594 (red), except for TUBB3, with which Alexa 488 (green) was used.



defined medium and the collapse, which is caused by utilizing only thermo-reversible physical gelation and would lead to being insufficient for preventing cells agglomeration. Most important of all, the introduction of thermo-reversible cross-linkage to the covalently cross-linked networks equip the final 3D cogelation microniche culture system with specific thermo-reversible degradation capability, which precisely enables the system to achieve a controlled release of the expanded cells by only changing the temperature. This dramatically simplifies the process of cells harvesting. Overall, this work provides an advanced, controlled release, defined, artificial niche engineering approach based on the physical–chemical-cogelation strategy that shows great promise in the field of iPSCs' 3D culture.

## 4. Experimental Section

**General Information:** Both PEG with Mw 6000 Dalton and poly(ethylene glycol)-acrylate with Mw 360 Dalton were purchased from RAPP Polymer (Germany). NIPAAm was purchased from Aldrich (Steinheim, Germany) and further purified by recrystallization from hexanes and dried under high vacuum for over 2 days (yield 80%). 2,2'-azobis(isobutyronitrile) (AIBN) was recrystallized from methanol before use. Anhydrous solvents  $\text{CH}_2\text{Cl}_2$ , THF, and toluene were taken from MBraun MB SPS-800 solvent purification system. Dialysis tubes (MWCO 2kDa) and prewetted RC tubing (MWCO 1kDa) were purchased from Aldrich (Steinheim, Germany). Cell counting kit-8 (CCK-8) assay, cell lysis buffer (16189), and Cell Light fluorescent protein labeling (red) for mitochondria were bought from Thermo Fisher. dPG with a number average molecular weight (Mn) of 5 kDa and a degree of branching of 64% was synthesized by procedure reported previously and characterized by size-exclusion chromatography (GPC).<sup>64</sup> NMR spectra were measured on a Jeol ECX 400 or Jeol ECP 500 MHz and 100 MHz spectrometer. IR spectra were recorded with a Nicolet AVATAR 320 FT-IR 5 SXC (Waltham, MA, USA) with a DTGS detector from 4000 to 650  $\text{cm}^{-1}$ . Morphology of the hydrogel niches was recorded with a SEM (SU8030, Hitachi, Germany). Optical and fluorescence micrographs of all the resultant microniche particles with cells encapsulated inside were recorded on a ZEISS fluorescence microscope. The cell viability was measured using a TECAN Infinite M200 Pro microplate reader. Confocal laser scanning microscopy was recorded by Leica TCS SP8 and disposed by Leica confocal software.

**Synthesis of Poly(*N*-Isopropylacrylamide)-co-Poly(ethylene Glycol):** The biocompatible pNIPAAm-co-PEG polymers were synthesized by chain reaction polymerization with NIPAAm and poly(ethylene glycol)-acrylate under the initiator molecule of AIBN. The synthesis process for this linker was according to the free-radical polymerization with some optimization.<sup>65</sup> To a flask filled with argon, NIPAAm (7.47 g, 66 mmol) and PEG-acrylate (4.75g, 13.2 mmol) were dissolved in 10 mL THF. Then, the flask was filled with argon again and 394 mg AIBN (dissolved in 5 mL THF) was injected by pumping under fierce stirring. The reaction was carried out at 65 °C, in dark and under stirring. After 24 h, the reaction mixture was precipitated directly in ice-cold  $\text{Et}_2\text{O}$  and colorless product was obtained by suction filtration. The copolymer was then dialyzed for 3 days, frozen, and lyophilized as a white solid (9.1 g, yield 72%). Formation and the purity of the pNIPAAm-co-PEG polymer was confirmed by  $^1\text{H}$  NMR (Figure S7, Supporting Information),  $^{13}\text{C}$  NMR (Figure S8, Supporting Information), and the element analysis test (Table S1, Supporting Information). For the desired-above product, NMR test ( $^1\text{H}$  NMR [500 MHz,  $\text{D}_2\text{O}$ ]  $\delta$  [ppm]: Figure S7, Supporting Information,  $^{13}\text{C}$  NMR [126 MHz,  $\text{D}_2\text{O}$ ]  $\delta$  [ppm]: Figure S8, Supporting Information), and the element analysis test (Table S2, Supporting Information), were done for characterization, showing successful purification. The mole ratio of NIPAAm and PEG (4.88:1  $\approx$  5:1) was calculated from the integration

ratio between the methyl protons (6 H for  $(\text{CH}_3)_2\text{CHNHCO-}$ ) of NIPAAm and the methylene protons (2H for  $\text{HOCH}_2\text{CH}_2(\text{OCH}_2\text{CH}_2)_n\text{OCH}_2\text{CH}_2\text{OCO-}$ ) of PEG appearing at 1.07 and 4.19 ppm (Figure S1, Supporting Information), respectively.

**Synthesis of Poly(*N*-Isopropylacrylamide)-co-Poly(ethylene Glycol Azide):** pNIPAAm-co-PEG (5g, 5.38 mmol  $-\text{OH}$ ) was first dried and then dissolved into DMF (100 mL) in a flask under fierce stirring. After that,  $\text{Et}_3\text{N}$  (1.122 mL, 8.0725 mmol) was added into the solution and the flask was cooled down to 0 °C with an ice bath. MsCl (0.92 g, 8.07 mmol) dissolved in DMF (15 mL) was added dropwise to the suspension. The reaction was performed at room temperature overnight. The color of the mixture solution changed to yellow. The product was purified by dialysis (MWCO 1 kDa) against a mixture of water and methanol. After lyophilization, the product (pNIPAAm-co-PEG-OMs) was obtained as a white solid. The presence of mesyl groups was confirmed by  $^1\text{H}$  and  $^{13}\text{C}$  NMR (Figures S9 and S10, Supporting Information).  $\text{NaN}_3$  (3.50g, 53.82 mmol) was added into the solution of mesylated polymer in DMF. At 65 °C, the reaction was kept stirring for 2 days. DMF was evaporated and the obtained residues were purified by dialysis using 1 kDa MWCO membrane first in water–methanol mixture and then in water for 1 day. Azide-functionalized polymer was obtained after lyophilization of the obtained aqueous solution as a white solid (3.74 g, yield 74.77%).  $^1\text{H}$  NMR (500 MHz,  $\delta$  (ppm) was done at different temperatures (298–313 K) and as shown in Figure S1, Supporting Information. From the  $^1\text{H}$  NMR tests in different temperature, the signals of the copolymer disappeared when the temperature was up to the the copolymer's LCST. Therefore, from these tests at different temperatures, it could be inferred that the LCST of the synthetic pNIPAAm-co-PEG- $\text{N}_3$  was about 304 K (31 °C).  $^{13}\text{C}$  NMR (400 MHz,  $\text{D}_2\text{O}$ )  $\delta$  (ppm) was shown in Figure S11, Supporting Information. Additionally, IR (Figure S12, Supporting Information), GPC (Figures S13 and S14, Supporting Information), and elemental analysis (Table S3, Supporting Information) confirmed the formation and purity of the pNIPAAm-co-PEG- $\text{N}_3$  polymer.

**Synthesis of Dendritic Polyglycerol-Bicyclononyne:** The dPG-(BCN)<sub>6%</sub> was synthesized in four steps starting with dPG (Mn = 6 kDa, Figures S15 and S16, Supporting Information): mesylation, azidation, reduction of azides with  $\text{PPh}_3$ , and then coupling with the BCN derivative. Azide-functionalized dPG was synthesized in two steps, mesylation and substitution by azide following the procedure as reported before<sup>66</sup> (Figures S17 and S18, Supporting Information). Amine-functionalized dPG was synthesized by reducing the dPG<sub>10</sub>( $\text{N}_3$ )<sub>6%</sub> using  $\text{PPh}_3$  in THF- $\text{H}_2\text{O}$  following the procedure as reported before<sup>67</sup> (Figure S19, Supporting Information). Conversion of azide groups to amine was also confirmed by IR by disappearance of peaks at 2100  $\text{cm}^{-1}$  as shown in the Figure S20, Supporting Information. Finally, the dPG- $\text{NH}_2$  was reacted with bicyclo[6.1.0]non-4-yn-9ylmethyl (4-nitrophenyl) carbonate (BCN-PNP) and dPG-BCN was synthesized as shown in Figure S21, Supporting Information.

**Synthesis of Bicyclononyne-Arg(Pmc)-GlyAsp(OtBu)-D-Phe-Lys(Boc):** BCN-RGD was synthesized based on the modification of BCN with cyclic pentapeptide c[RGDFK], which was linked to BCN through its lysine residue without hindering its biological performance.<sup>60,68</sup> Cyclic Arg(Pmc)-GlyAsp(OtBu)-D-Phe-Lys(Boc) (60 mg, 0.0993 mmol) was dissolved in 24 mL DMF, followed by addition of TEA (48  $\mu\text{L}$ , 3 eq.). A solution of bicyclo[6.1.0]non-4-yn-9ylmethyl (4-nitrophenyl) carbonate (32.85 mg, 0.1143 mmol, 1.05 eq.) dissolved in 24 mL DMF was added into the RGD solutions and stirred for 16 h at room temperature. After that, the DMF was removed by rotary evaporator, and the residue was purified by column with ethyl acetate as eluent. After that 74.254 mg (80% yield) product was obtained.

**Artificial Niche Fabrication:** First, two sets of aqueous precursor solutions with different concentrations (Table S1, Supporting Information) were prepared by dissolving ultrapur precursors of pNIPAAm-co-PEG- $\text{N}_3$  and dPG-BCN (with BCN-RGD, and the final concentration of c[RGDFK] in precursors mixtures was kept as 1  $\text{mM}$ <sup>60</sup>) in cell medium separately. Together with (or without) iPSC cells in culture medium with varying densities, the pNIPAAm-co-PEG azide and dPG-BCN (with BCN-RGD) precursor solutions were mixed in EP tubes



under series of different parameters (concentrations and ratios). Then, the niches with cells seeded inside were immediately transferred from the EP pipe to the culture dish plates. After that, the culture dish plates were kept at room temperature for 20 min (chemical gelation happens by mechanism of SPAAC reaction). After addition of cell medium, the plates with niche gels were then transferred into carbon dioxide cell incubator at 37 °C (physical gelation happens). Finally, it formed a chemical and physical cogelation system inside the niche.

**Cell Culture:** The mouse iPSC cell line PhiC31 was obtained from System Biosciences (Catalog# SC211A-1). The iPSCs were usually maintained on plate coated with laminin (Cultrex, #3400-010-01) and cultured with complete clonal grade medium (Merck Millipore, #SF001-500P) containing GSK3 $\beta$  inhibitor at 37 °C with 5% CO<sub>2</sub>. The medium was usually changed daily and the cells were passaged every 3–4 days with Accutase (Merck Millipore, #SCR005). For iPSCs' 3D suspension culture, the cells were trypsinized with Accutase solution into single cells and then reseeded on uncoated plate with defined concentration. The medium was changed daily by gently centrifuging the cell spheroids into the bottom of the tubes and carefully aspirating the supernatant. For the 3D artificial niche culture, iPSC cells were trypsinized with Accutase into single cells and then carefully aspirating the supernatant to get certain cell concentration before ready to use.

**Controlled Release and Cell Harvest:** After being cultured for certain time (at 37 °C with 5% CO<sub>2</sub>), the cell expansion niche system could be transferred to room temperature (25 °C) conditions again for 5 min during which time the physical gelation disappeared and thus only chemical gelation was left in the niche system so that the niche was loosened, and expanded cells would release out of the niches. After centrifuging (400 r min<sup>-1</sup>) for 5 min, the pure cells were harvested.

**Spheroids' Size Distribution:** The cells in niche systems were imaged by normal or fluorescent microscope at specific time points and the cell spheroids' numbers and diameters were counted and measured by ImageJ software.

**Cell Viability:** The viability of iPSCs in different culture system was measured by live/dead assay using a Live/Dead Viability kit (Thermo Fisher #L3224). Briefly, the live/dead dye solution was prepared by mixing 5  $\mu$ L of  $4 \times 10^{-3}$  mol L<sup>-1</sup> calcein AM and 20  $\mu$ L of  $2 \times 10^{-3}$  mol L<sup>-1</sup> EthD-1 stock solution into 10 mL of Dulbecco's phosphate-buffered saline. A freshly prepared staining solution was added to niche system with cells inside or cells finally got from PBS and then cells or spheroids were stained in the dark. After incubation for 40 min at 37 °C under a rocking device, the cells or spheroids were imaged by SP8-confocal microscope. Cell viability could be indicated by the green-fluorescent calcein-AM (indicated live cells) and the red-fluorescent ethidium homodimer-1 (indicated live cells), especially by their ratio in the live/dead staining image. Besides the live/dead staining, cell viability could also be preliminarily indicated and monitored by the bright field microscope. Both of the cells in niche system or after released from the niche system could be monitored by their EB size distribution and frequency in different culture days, which could also be effective in indicating the cell viability and proliferation efficiency.

**Cell Proliferation:** Cell Counting Kit-8 (Sigma, #96992) was used to measure the expansion rate of the iPSC cells growing in different culture systems. Briefly, at the beginning of an indicated time period, one tenth of the volume of CCK-8 reagent of the cell culture medium was added to each well of the plate with cells, and then incubated at 37 °C for 2 h. After incubation, the supernatants were transferred to 96-well plate, and the OD value for each well was read at wavelength 450 nm to determine the cell viability on a microplate reader. The assay was repeated thrice. The cell viability was calculated as following: cell viability (%) = (OD [experiment] – OD [blank]) / (OD [control] – OD [blank]  $\times$  100).

**Immunofluorescent Staining:** After being released from the niche system at specified time periods, the cells were collected and washed with PBS (with 0.1% TritonX-100). Then the cells were fixed with 4% paraformaldehyde (PFA) (0.5% TritonX-100 in PBS) to fix them for 15–30 min, which was followed by permeabilization for 10–50 min (bigger cell spheroids need longer time). After washing with PBS for three times (putting on shaker rocking for 3 min each time), the cells were blocked

with 1 mL 10% goat serum at 4 °C for overnight to cover nonspecific sites. Then they were incubated with defined primary antibodies in PBS with 0.1% TritonX-100 (anti-Nanog, 1:300, Abcam, #ab80892; anti-Sox2, 1:400, CST, #4900; anti-Oct4, 1:500, Abcam, #ab19857; anti-SSEA1, 1:300, Thermo Fisher, #MA1-022; anti-Ki-67, 1:400, CST, #9129) at 4 °C overnight. At least one blank sample was used as a negative control in these tests. Cells were washed again with PBS for three times the 2nd day and then incubated with secondary antibodies (goat anti-rabbit IgG H&L (Alexa Fluor 488), 1:400, Abcam, #ab150077; goat anti-mouse IgG H&L (Cy5), 1:1000, Abcam, #ab6563) under a dark environment at 37 °C for 1 h. After that, the cells were washed with PBS and stained with DAPI (1:2000) at room temperature for 30–40 min. Finally, after washing with PBS, the cells were imaged by sp8 confocal microscope.

**Alkaline Phosphatase Staining:** To confirm the pluripotency of iPSCs, ALP staining was performed by following the instructions of an ALP detection kit (Merck Millipore, #SCR004). Briefly, after collected and washed by PBS, cells spheroids were fixed by 4% PFA for very short time followed by PBS washing again. Then, they were transferred to the stain solution and then incubated at room temperature in dark for 15 min. After thrice washing with PBS, the images were observed and acquired by a color microscope.

**In Vitro Differentiation of Induced Pluripotent Stem Cells:** After 3 days' culture, cells were harvested and transferred onto gelatin-coated tissue culture dishes and also in the ESGRO medium without Gsk3 $\beta$  inhibitor and incubated for another 3 days. The cells were washed with PBS for 30 min and fixed with 4% PFA for 30 min at room temperature. Fixed cells were washed thrice with PBS and permeabilized in 0.5% Triton X-100 for 30 min at room temperature. Permeabilized cells were then blocked with 10% goat serum overnight at 4 °C. Cells were stained overnight with primary antibody at 4 °C. After three PBS washes, cells were stained with corresponding secondary antibody (1:1000; Invitrogen) overnight at 4 °C in the dark. Cells were washed thrice with PBS and incubated for 30 min in 4',6-diamidino-2-phenylindole (Invitrogen) for nuclei visualization. Confocal imaging was carried out using SP8 (Leica). The follows antibodies were used:  $\beta$  III tubulin (D71G9) Rabbit mAb (neuroectodermal marker, Cell signaling 5568T, 1:200), anti-smooth muscle actin (D4K9N) monoclonal Rabbit antibody (mesodermal marker, Cell signaling, 19245T, 1:200), and Rabbit anti-FOXA2 polyclonal antibody (Millipore, ref. no. AB4125, 1:200), goat anti-rabbit IgG H&L (Alexa Fluor 488, 1:1000, Abcam, #ab150077), and goat anti-rabbit IgG H&L (Alexa Fluor 594, Thermo Fisher, #A-11012, 1:1000).

**Scanning Electron Microscopy Imaging:** The niche gels formed by pNIPAAm-co-PEG azide and dPG-BCN were first put in a cell culture media overnight for swelling absolutely. After washing with PBS, the swollen niche gels were freeze-dried and then gold-sputtered for 30 s with gold deposition rate of 15 nm min<sup>-1</sup>. SEM characterized the morphologies of niches.

**Rheology:** Rheological data were measured with a Malvern Instruments Kinexus equipped with a parallel plate geometry (PU08:PL65) and with an 8 mm plate-plate. The plate gap was set as 0.2 mm and the temperature was kept at 25 °C for all experiments with an average normal force of  $\approx$ 0.07 N. For the amplitude sweep, the scan range was set as 0.01–10% at 1 Hz. For frequency sweep, the frequency scan range was set as 0–10 Hz at 1%. All rheological experiments were repeated thrice.

## Supporting Information

Supporting Information is available from the Wiley Online Library or from the author.

## Acknowledgements

W.J.L. gratefully acknowledges financial support from the China Scholarship Council. The authors would like to acknowledge the

assistance of the SFB 765 of the Deutsche Forschungsgemeinschaft (DFG), Dr. Anke Schindler for SEM tests, Anja Stösel for dPG synthesis and GPC test, and Dr. Pamela Winchester for language polishing this manuscript.

Open access funding enabled and organized by Projekt DEAL.

## Conflict of Interest

The authors declare no conflict of interest.

## Data Availability Statement

Research data are not shared.

## Keywords

dendritic polyglycerol, induced pluripotent stem cells, physical-chemical cogelation, poly(*N*-isopropylacrylamide)-*co*-polyethylene glycol, three-dimensional artificial niches

Received: December 10, 2020

Revised: May 25, 2021

Published online: July 10, 2021

- [1] K. Takahashi, S. Yamanaka, *Cell* **2006**, 126, 663.
- [2] R. Shrestha, *Prog. Stem Cell* **2020**, 7, 296.
- [3] K. Takahashi, S. Yamanaka, *Development* **2013**, 140, 2457.
- [4] M. Scudellari, *Nature* **2016**, 534, 310.
- [5] M. X. Doss, A. Sachinidis, *Cells* **2019**, 8, 403.
- [6] M. Bellin, M. C. Marchetto, F. H. Gage, C. L. Mummery, *Nat. Rev. Mol. Cell Biol.* **2012**, 13, 713.
- [7] D. Doi, H. Magotani, T. Kikuchi, M. Ikeda, S. Hiramatsu, K. Yoshida, N. Amano, M. Nomura, M. Umekage, A. Morizane, J. Takahashi, *Nat. Commun.* **2020**, 11, 3369.
- [8] C. Yamashiro, K. Sasaki, S. Yokobayashi, Y. Kojima, M. Saitou, *Nat. Protoc.* **2020**, 15, 1560.
- [9] A. D. Baldassarre, E. Cimetta, S. Bollini, G. Gaggi, B. Ghinassi, *Cells* **2018**, 7, 48.
- [10] Y. Hayashi, M. Takami, M. M. Takasaki, *Front. Cell. Neurosci.* **2020**, 4, 224.
- [11] R. N. Judson, M. V. Rossi, *npj Regener. Med.* **2020**, 5, 10.
- [12] C. M. Fan, E. Zhang, J. Joshi, J. F. Yang, J. Y. Zhang, W. Q. Zhu, *Front. Cell Dev. Biol.* **2020**, 8, 36.
- [13] M. Serra, C. Brito, C. Correia, P. M. Alves, *Trends Biotechnol.* **2012**, 30, 350.
- [14] Y. Fan, J. Wu, P. Ashok, M. Hsiung, E. S. Tzanakakis, *Stem Cell Rev. Rep.* **2015**, 11, 96.
- [15] H. Zhan, D. W. P. M. Löwik, *Adv. Funct. Mater.* **2019**, 29, 1808505.
- [16] I. Chimenti, D. Massai, U. Morbiducci, A. P. Beltrami, M. Pesce, E. Messina, *J. Cardiovasc. Transl. Res.* **2017**, 10, 150.
- [17] M. W. Lensch, L. Daheron, T. M. Schlaeger, *Stem Cell Rev.* **2006**, 2, 185.
- [18] D. Jhala, R. Vasita, *Polym. Rev.* **2015**, 55, 561.
- [19] A. J. Want, A. W. Nienow, C. J. Hewitt, K. Coopman, *Regener. Med.* **2012**, 7, 71.
- [20] L. G. Villa-Diaz, A. M. Ross, J. Lahann, P. H. Krebsbach, *Stem Cells* **2013**, 31, 1.
- [21] L. Liu, K. I. Kamei, M. Yoshioka, M. Nakajima, J. Li, N. Fujimoto, S. Terada, Y. Tokunaga, Y. Koyama, H. Sato, K. Hasegawa, N. Nakatsuji, Y. Chen, *Biomaterials* **2017**, 124, 47.
- [22] F. C. P. Mesquita, C. Hochman-Mendez, J. Morrissey, L. C. Sampaio, D. A. Taylor, *Stem Cells Int.* **2019**, 2019, 9704945.
- [23] J. Thiele, Y. Ma, S. M. C. Bruekers, S. Ma, W. T. Huck, *Adv. Mater.* **2014**, 26, 125.
- [24] M. Bao, J. Xie, W. T. S. Huck, *Adv. Sci.* **2018**, 5, 1800448.
- [25] K. G. Chen, B. S. Mallon, R. D. McKay, P. G. Robey, *Cell Stem Cell* **2014**, 14, 13.
- [26] R. Cruz-Acuna, M. Quiros, A. E. Farkas, P. H. Dedhia, S. Huang, D. Siuda, V. Garcia-Hernandez, A. J. Miller, J. R. Spence, A. Nusrat, A. J. Garcia, *Nat. Cell Biol.* **2017**, 19, 1326.
- [27] K. R. Stevens, C. E. Murry, *Cell Stem Cell* **2018**, 22, 294.
- [28] S. P. Pasca, *Nature* **2018**, 553, 437.
- [29] N. Gjorevski, N. Sachs, A. Manfrin, S. Giger, M. E. Bragina, P. Ordóñez-Moran, H. Clevers, M. P. Lutolf, *Nature* **2016**, 539, 560.
- [30] M. P. Lutolf, P. M. Gilbert, H. M. Blau, *Nature* **2009**, 462, 433.
- [31] A. M. Akimoto, E. H. Niitsu, K. Nagase, T. Okano, H. Kanazawa, R. Yoshida, *Int. J. Mol. Sci.* **2018**, 19, 1253.
- [32] T. C. Sunga, H. F. Li, A. Higuchi, S. S. Kumarg, Q. D. Lingh, Y. W. Wui, T. Burnouf, M. Nasud, A. Umezawad, K. F. Leel, H. C. Wangm, Y. Change, S. T. Hsun, *Biomaterials* **2020**, 230, 119638.
- [33] S. M. Vornholt, R. E. Morris, *Nat. Mater.* **2019**, 18, 910.
- [34] I. C. Yasa, A. F. Tabak, O. Yasa, H. Ceylan, M. Sitti, *Adv. Funct. Mater.* **2019**, 29, 1808992.
- [35] J. Koh, D. R. Griffin, M. M. Archang, A. C. Feng, T. Horn, M. Margolis, D. Zalazar, T. Segura, P. O. Scumpia, D. Di Carlo, *Small* **2019**, 15, 1903147.
- [36] R. Y. Chen, L. Li, L. Feng, Y. X. Luo, M. E. Xu, K. W. Leong, R. Yao, *Biomaterials* **2020**, 230, 119627.
- [37] D. Seliktar, *Science* **2012**, 336, 1124.
- [38] E. Prince, E. Kumacheva, *Nat. Rev. Mater.* **2019**, 4, 99.
- [39] M. Caiazzo, Y. Okawa, A. Ranga, A. Piersigilli, Y. Tabata, M. P. Lutolf, *Nat. Mater.* **2016**, 15, 344.
- [40] F. M. Chen, X. Liu, *Prog. Polym. Sci.* **2016**, 53, 86.
- [41] D. Steinhilber, T. Rossow, S. Wedepohl, F. Paulus, S. Seiffert, R. Haag, *Angew. Chem., Int. Ed.* **2013**, 52, 13538.
- [42] Y. Lei, D. V. Schaffer, *Proc. Natl. Acad. Sci. USA* **2013**, 110, E5039.
- [43] B. L. Seala, T. C. Oterob, A. Panitcha, *Mater. Sci. Eng., R* **2001**, 34, 147.
- [44] P. Zhou, B. Yin, R. Zhang, Z. Xu, Y. Liu, Y. Yan, X. Zhang, S. Zhang, Y. Li, H. Liu, Y. A. Yuan, S. Wei, *Colloids Surf., B* **2018**, 171, 451.
- [45] I. Lilge, H. Schonherr, *Angew. Chem., Int. Ed.* **2016**, 55, 13114.
- [46] T. Scholzen, J. Gerdes, *J. Cell. Physiol.* **2000**, 182, 311.
- [47] J. Tu, G. Tian, H. H. Cheung, W. Wei, T. L. Lee, *Stem Cell Res. Ther.* **2018**, 9, 71.
- [48] Y. Zhou, H. Mao, B. Joddar, N. Umeki, Y. Sako, K.-I. Wada, C. Nishioka, E. Takahashi, Y. Wang, Y. Ito, *Sci. Rep.* **2015**, 5, 11386.
- [49] D. Thomas, T. O'Brien, A. Pandit, *Adv. Mater.* **2018**, 30, 1703948.
- [50] K. H. Vining, A. Stafford, D. J. Mooney, *Biomaterials* **2019**, 188, 187.
- [51] S. Talebian, M. Mehrali, N. Taebnia, C. P. Pennisi, F. B. Kadumudi, J. Foroughi, M. Hasany, M. Nikkhah, M. Akbari, A. G. Orive, A. D. Pirouz, *Adv. Sci.* **2019**, 6, 1801664.
- [52] M. Sofman, A. Brown, L. G. Griffith, P. T. Hammond, *Biomaterials* **2021**, 264, 120231.
- [53] J. Zhang, H. Yang, B. E. Abali, M. Li, Y. Xia, R. Haag, *Small* **2019**, 15, 1901920.
- [54] H. G. Schild, *Prog. Polym. Sci.* **1992**, 17, 163.
- [55] T. Sun, G. Qing, *Adv. Mater.* **2011**, 23, H57.
- [56] J. Zhang, C. Cheng, J. L. Cuellar-Camacho, M. Li, Y. Xia, W. Li, R. Haag, *Adv. Funct. Mater.* **2018**, 28, 1804773.
- [57] M. Jaspers, S. L. Vaessen, P. van Schayik, D. Voerman, A. E. Rowan, P. H. J. Kouwer, *Nat. Commun.* **2017**, 8, 15478.
- [58] B. Trappmann, C. S. Chen, *Curr. Opin. Biotechnol.* **2013**, 24, 948.
- [59] B. Trappmann, J. E. Gautrot, J. T. Connelly, D. G. Strange, Y. Li, M. L. Oyen, M. A. C. Stuart, H. Boehm, B. Li, V. Vogel, J. P. Spatz, F. M. Watt, W. T. Huck, *Nat. Mater.* **2012**, 11, 642.
- [60] S. B. Anderson, C. C. Lin, D. V. Kuntzler, K. S. Anseth, *Biomaterials* **2011**, 32, 3564.

- [61] P. M. Kharkar, K. L. Kiick, A. M. Kloxin, *Chem. Soc. Rev.* **2013**, *42*, 7335.
- [62] T. E. Brown, I. A. Marozas, K. S. Anseth, *Adv. Mater.* **2017**, *29*, 1605001.
- [63] J. Lai, L. Abune, N. Zhao, Y. Wang, *Angew. Chem., Int. Ed.* **2019**, *58*, 2820.
- [64] R. Haag, H. Türk, S. Mecking, *German patent application DE10211664A1*, **2003**.
- [65] V. Cheng, B. H. Lee, C. Pauken, B. L. Vernon, *J. Appl. Polym. Sci.* **2007**, *106*, 1201.
- [66] S. Bhatia, D. Lauster, M. Bardua, K. Ludwig, S. Angioletti-Uberti, N. Popp, U. Hoffmann, F. Paulus, M. Budt, M. Stadtmuller, T. Wolff, A. Hamann, C. Bottcher, A. Herrmann, R. Haag, *Biomaterials* **2017**, *138*, 22.
- [67] S. Roller, H. Zhou, R. Haag, *Mol. Diversity* **2005**, *9*, 305.
- [68] F. Stijn, M. Dongen, *Adv. Mater.* **2013**, *25*, 1687.